



Supplement of

Mixing times of organic molecules within secondary organic aerosol particles: a global planetary boundary layer perspective

Adrian M. Maclean et al.

Correspondence to: Allan K. Bertram (bertram@chem.ubc.ca) and Jose L. Jimenez (jose.jimenez@colorado.edu)

The copyright of individual parts of the supplement might differ from the CC BY 3.0 License.

Supporting Information

S1. Calculations of vertical profiles of temperature and RH in the boundary layer above Hyytiälä (boreal forest) and the Amazon (rainforest)

The monthly average afternoon (13:00-15:00, local time) temperature and RH vertical profiles over Hyytiälä and the Amazon were calculated for the driest month of the year at these locations. For Hyytiälä, the average afternoon temperatures and RHs at the surface were obtained from the SMEAR II campaign data set for 2012, retrieved from Etsin Research data finder (<https://etsin.avointiede.fi/dataset>) (Aalto, 2012a, 2012b). For the Amazon, the temperature and RH at the surface were obtained from NOAA's National Climate Data Center (<http://www.ncdc.noaa.gov/>) from 2004 to 2014, and an average from five different stations was used (Alfredo Vasquez Cobo, Itaituba, Tabatinga, Monte Dourado and Iauarete).

The vertical profiles of temperature were calculated using a dry adiabatic lapse rate of 9.8 K km^{-1} and the average afternoon surface temperatures mentioned above. The vertical profiles of RH were calculated using the average afternoon surface RHs mentioned above, the vertical profiles of temperature (calculated with the dry adiabatic lapse rate), and assuming the mixing ratio of water is independent of height in the PBL. For the calculations of RH as a function of altitude, the water vapor pressure and water saturated vapour pressure were needed as a function of altitude. The water vapor pressure as a function of altitude was determined by multiplying the mixing ratio of water by the atmospheric pressure, calculated using the following equation (Seinfeld and Pandis, 2006):

$$P(z) = P_0 \exp\left(-\frac{Mgz}{kT}\right) \quad (\text{S1})$$

where P_0 is the standard pressure at sea level (101325 Pa), M is the molecular mass of the air (28.8 g/mol), g is the acceleration due to gravity (9.81 m s^{-2}), z is the altitude in metres, k is the Boltzmann constant and T is the temperature in Kelvin. The water saturated vapour pressure was calculated as a function of attitude using the Antoine equation (National Institute of Standards and Technology, 2016):

$$\log_{10}(P) = A - \left(\frac{B}{T+C}\right) \quad (\text{S2})$$

where P is the pressure, $A=4.6543$, $B=1435.264$, $C=-64.848$ and T is the temperature in Kelvin. The values for A , B and C were based on the NIST values for water, which are valid for temperatures between 256 and 373 K (National Institute of Standards and Technology, 2016).

In Fig. 5, the temperature and RH were plotted until the RH reached 100 %. The height at which RH reached 100 % was only slightly lower than the average height of the planetary boundary layer predicted by GEOS-5 meteorology data for the driest month of the year and for the afternoon (13:00-15:00, local time) above Hyytiälä and the Amazon. For Hyytiälä, 100 % RH was reached

at 1605 m, while GEOS-5 predicted an average height of the PBL of 1667 m for this location and time. For the Amazon, 100 % RH was reached at 882 m, while GEOS-5 predicted an average height of the PBL of 1249 m for this location and time. When predicting the height of the PBL using GEOS-5 meteorology, we ran GEOS-Chem at a horizontal grid resolution of 2° latitude by 2.5° longitude rather 4° latitude by 5° longitude to provide a better approximation to these single locations.

S2. Parametrization for the viscosity of sucrose particles as a function of temperature and RH

We developed a parameterization for viscosity of sucrose particles as function of temperature and RH by fitting the viscosity data listed in Table S7 to the following equation:

$$\log(\eta) = 12 - \frac{C_1 * (T - \frac{w_{Suc} T_{gSuc} + w_{H2O} T_{gH2O} k_{GT}}{w_{Suc} + w_{H2O} k_{GT}})}{C_2 + (T - \frac{w_{Suc} T_{gSuc} + w_{H2O} T_{gH2O} k_{GT}}{w_{Suc} + w_{H2O} k_{GT}})} \quad (S3)$$

where C_1 and C_2 are constants, k_{GT} is the Gordon-Taylor fitting parameter, T_{gSuc} and T_{gH2O} are the glass transition temperatures of dry sucrose and water and w_{Suc} and w_{H2O} are the weight fractions of the dry sucrose and water in the particles. The weight fractions of dry sucrose and water in the particles were determined from the RH using the following equation (Zobrist et al., 2011):

$$\frac{RH}{100} = \frac{1 + aw_{Suc}}{1 + bw_{Suc} + cw_{Suc}^2} + (T - T^\theta)(dw_{Suc} + ew_{Suc}^2 + fw_{Suc}^3 + gw_{Suc}^4) \quad (S4)$$

where a-g are fitting parameters, T is the temperature in Kelvin and T^θ is a reference temperature. The values for T^θ and a-g can be found in Table S8.

When fitting Eq. (S3) to the viscosity data for sucrose (Table S7), the parameters C_1 , C_2 , k_{GT} and T_{gSuc} were included as fitting parameters, while the glass transition temperature of water was fixed at 135 K (Longinotti and Corti, 2008). The values for these parameters retrieved by fitting are reported in Table S9. The T_{gSuc} value obtained by fitting was within the range measured experimentally (319-335K) (Dette et al., 2014; Roos, 1993; Simperler et al., 2006).

Equation (S3) was based on the Williams, Landel and Ferry (WLF) equation and the Gordon-Taylor equation, similar to Eq. (1) in the main text. Since the WLF equation is only valid at or above the glass transition temperature, we have not used Eq. (S3) to predict viscosities above 10^{12} Pa s (which corresponds to mixing times longer than 5×10^5 h) (Fig. S7). If the temperature and RH in the PBL were such that the viscosity was greater than 10^{12} Pa s, we assigned a viscosity of 10^{12} Pa s and a mixing time of 5×10^5 hours. This assignment does not affect the conclusions in this manuscript since a mixing time of 5×10^5 hours is already well above the residence time of SOA particles in the atmosphere. However, this assignment did lead to a relatively large frequency count at 5×10^5 hours in Fig. S9.

References

- Aalto, P.: Hyytiälä SMEAR II meteorology, gases and soil- Air temperature 8.4 m- 2012, atm-data@helsinki.fi, Etsin Res. data finder [online] Available from: <http://urn.fi/urn:nbn:fi:csc-kata20160308104539432017> (Accessed 28 June 2016a), 2012.
- Aalto, P.: Hyytiälä SMEAR II meteorology, gases and soil- Relative humidity 16 m-2012, atm-data@helsinki.fi, Etsin Res. data finder [online] Available from: <http://urn.fi/urn:nbn:fi:csc-kata20160308112058571248> (Accessed 28 June 2016b), 2012.
- Crittenden, J. C., Trussel, R. R., Hand, D. W., Howe, K. J. and Tchobanoglous, G.: MWH's Water Treatment, John Wiley and Sons., 2012.
- Detle, H. P., Qi, M. A., Schroder, D. C., Godt, A. and Koop, T.: Glass-Forming Properties of 3-Methylbutane-1,2,3-tricarboxylic Acid and Its Mixtures with Water and Pinonic Acid, *J. Phys. Chem. A*, 118(34), 7024–7033, doi:10.1021/jp505910w, 2014.
- Först, P., Werner, F. and Delgado, A.: On the pressure dependence of the viscosity of aqueous sugar solutions, *Rheol. Acta*, 41(4), 369–374, doi:10.1007/s00397-002-0238-y, 2002.
- Grayson, J. W., Zhang, Y., Mutzel, A., Renbaum-Wolff, L., Boege, O., Kamal, S., Herrmann, H., Martin, S. T. and Bertram, A. K.: Effect of varying experimental conditions on the viscosity of alpha-pinene derived secondary organic material, *Atmos. Chem. Phys.*, 16(10), 6027–6040, doi:10.5194/acp-16-6027-2016, 2016.
- Järvinen, E., Ignatius, K., Nichman, L., Kristensen, T. B., Fuchs, C., Hoyle, C. R., Höppel, N., Corbin, J. C., Craven, J., Duplissy, J., Ehrhart, S., El Haddad, I., Frege, C., Gordon, H., Jokinen, T., Kallinger, P., Kirkby, J., Kiselev, A., Naumann, K. H., Petäjä, T., Pinterich, T., Prevot, A. S. H., Saathoff, H., Schiebel, T., Sengupta, K., Simon, M., Slowik, J. G., Tröstl, J., Virtanen, A., Vochezer, P., Vogt, S., Wagner, A. C., Wagner, R., Williamson, C., Winkler, P. M., Yan, C., Baltensperger, U., Donahue, N. M., Flagan, R. C., Gallagher, M., Hansel, A., Kulmala, M., Stratmann, F., Worsnop, D. R., Möhler, O., Leisner, T. and Schnaiter, M.: Observation of viscosity transition in α -pinene secondary organic aerosol, *Atmos. Chem. Phys.*, 16(7), 4423–4438, doi:10.5194/acp-16-4423-2016, 2016.
- Longinotti, M. P. and Corti, H. R.: Viscosity of concentrated sucrose and trehalose aqueous solutions including the supercooled regime, *J. Phys. Chem. Ref. Data*, 37(3), 1503–1515, doi:10.1063/1.2932114, 2008.
- Migliori, M., Gabriele, D., Di Sanzo, R., De Cindio, B. and Correra, S.: Viscosity of multicomponent solutions of simple and complex sugars in water, *J. Chem. Eng. Data*, 52(4), 1347–1353, doi:10.1021/je700062x, 2007.
- National Institute of Standards and Technology: Water, [online] Available from: <http://webbook.nist.gov/cgi/cbook.cgi?ID=C7732185&Mask=4&Type=ANTOINE&Plot=on#ANTOINE> (Accessed 1 August 2016), 2016.
- Perry, R. and Green, D.: Perry's Chemical Engineers' Handbook, McGraw-Hill, Toronto., 2008.
- Power, R. M. and Reid, J. P.: Probing the micro-rheological properties of aerosol particles using optical tweezers, *Reports Prog. Phys.*, 77(7), doi:10.1088/0034-4885/77/7/074601, 2014.
- Quintas, M., Brandão, T. R. S., Silva, C. L. M. and Cunha, R. L.: Rheology of supersaturated sucrose solutions, *J. Food Eng.*, 77(4), 844–852, doi:10.1016/j.jfoodeng.2005.08.011, 2006.

- Roos, Y.: Melting and glass transitions weight carbohydrates of low molecular, Carbohydr. Res., 238, 39–48, doi:10.1016/0008-6215(93)87004-C, 1993.
- Seinfeld, J. H. and Pandis, S. N.: Atmospheric Chemistry and Physics, 2nd Ed., John Wiley and Sons, Hoboken, NJ., 2006.
- Simperler, A., Kornherr, A., Chopra, R., Bonnet, P. A., Jones, W., Motherwell, W. D. S. and Zifferer, G.: Glass transition temperature of glucose, sucrose, and trehalose: An experimental and in silico study, J. Phys. Chem. B, 110(39), 19678–19684, doi:10.1021/jp063134t, 2006.
- Song, M. J., Liu, P. F. F., Hanna, S. J., Zaveri, R. A., Potter, K., You, Y., Martin, S. T. and Bertram, A. K.: Relative humidity-dependent viscosity of secondary organic material from toluene photo-oxidation and possible implications for organic particulate matter over megacities, Atmos. Chem. Phys., 16(14), 8817–8830, doi:10.5194/acp-16-8817-2016, 2016.
- Swindells, J. F. and States., U.: Viscosities of sucrose solutions at various temperatures: tables of recalculated values, , 7 [online] Available from: file://catalog.hathitrust.org/Record/007290919, 1958.
- Telis, V. R. N., Telis-Romero, J., Mazzotti, H. B. and Gabas, a. L.: Viscosity of Aqueous Carbohydrate Solutions at Different Temperatures and Concentrations, Int. J. Food Prop., 10(1), 185–195, doi:10.1080/10942910600673636, 2007.
- Zhang, Y., Sanchez, M. S., Douet, C., Wang, Y., Bateman, A. P., Gong, Z., Kuwata, M., Renbaum-Wolff, L., Sato, B. B., Liu, P. F., Bertram, A. K., Geiger, F. M. and Martin, S. T.: Changing shapes and implied viscosities of suspended submicron particles, Atmos. Chem. Phys., 15(14), 7819–7829, doi:10.5194/acp-15-7819-2015, 2015.
- Zobrist, B., Marcolli, C., Pedernera, D. A. and Koop, T.: Do atmospheric aerosols form glasses?, Atmos. Chem. Phys., 8(17), 5221–5244, doi:10.5194/acp-8-5221-2008, 2008.
- Zobrist, B., Soonsin, V., Luo, B. P., Krieger, U. K., Marcolli, C., Peter, T. and Koop, T.: Ultra-slow water diffusion in aqueous sucrose glasses, Phys. Chem. Chem. Phys., 13(8), 3514–3526, doi:10.1039/c0cp01273d, 2011.

Tables

Table S1. Room-temperature α -pinene SOA viscosity data from Grayson et al. (2016). Viscosity data corresponds to SOA generated with a mass concentration of $520 \mu\text{g m}^{-3}$.

Reference	Viscosity (Pa s)	RH (%)	Temperature (K)
Grayson et al. (2016) (SOA generated with a mass concentration = $520 \mu\text{g m}^{-3}$)	^a Range= 4.2×10^2 – 3.1×10^4 , midpoint= 3.6×10^3	50	^c Range=293– 295 Midpoint=294
	^a Range= 9.7×10^2 – 7.9×10^4 , midpoint= 8.7×10^3	40	
	^a Range= 3.4×10^3 – 2.1×10^5 , midpoint= 2.6×10^4	30	
	^a Range= 3.5×10^5 – 1.8×10^7 , midpoint= 2.5×10^6	^b 0	

^a Grayson et al. (2016) reported upper and lower limits to the viscosity (i.e. range) at each specified RH. To simplify the fitting procedure, we used the midpoints of the viscosities from Grayson et al (2016).

^b Grayson et al. (2016) measured the viscosity under dry conditions (RH of < 0.5 % based on measurements). When developing the parameterization, we used a value of 0 % RH.

^c Grayson et al. (2016) carried out experiments at room temperature (293 K-295 K). We used the midpoint of the temperature (294 K) when developing the viscosity parameterization for α -pinene SOA.

Table S2. Low-temperature α -pinene SOA viscosity data from Järvinen et al. (2016). Viscosity data corresponds to SOA generated with a mass concentration of 707-1414 $\mu\text{g m}^{-3}$.

Reference	Viscosity (Pa s)	RH (%)	Temperature (K)
Järvinen et al. (2016)	1×10^7	^a Range=22.9-36.3, midpoint=29.6	263.3
		^a Range=30.5-37.3, midpoint=33.9	262.9
		^a Range=40.5-46.0, midpoint=43.3	253.3
		^a Range=44.0-49.8, midpoint=46.9	252.9
		^a Range=55.0-63.4, midpoint=59.2	243.3
		^a Range=68.6-80.1, midpoint=74.4	235.5

^a Järvinen et al (2016) reported upper and lower limits to the RH for a specific temperature and viscosity. To simplify fitting, we used the midpoint of the RH range.

Table S3. Liquid water viscosity data from Crittenden et al. (2012).

Reference	Viscosity (Pa s)	RH (%)	Temperature (K)
Crittenden et al. (2012)	^a 1.002 $\times 10^{-3}$	100	293
	^a 1.139 $\times 10^{-3}$		288
	^a 1.307 $\times 10^{-3}$		283
	^a 1.518 $\times 10^{-3}$		278
	^a 1.781 $\times 10^{-3}$		273

^a The viscosity values in Crittenden et al. (2012) were reported to 4 significant digits.

Table S4. Initial guess parameters and fitting parameters used in Eq. (1) to predict the viscosity of α -pinene SOA as a function of temperature and RH. The fitting parameters were obtained by fitting Eq. (1) to the viscosity data listed in Tables S1-S3.

Parameter	Guess Value	Fitting Value
C_1	19	131
C_2	50 K	1165 K
K_{GT}	2.5	3.934
T_{gSOA}	250 K	236.8 K

Table S5. Room temperature α -pinene SOA viscosity data from Zhang et al. (2015). Viscosity data corresponds to SOA generated with a mass concentration of $\sim 70 \mu\text{g m}^{-3}$.

Reference	Viscosity (Pa s)	RH (%)	Temperature (K)
Zhang et al. (2015) ^a	2.3×10^8	5.2	293
	1.3×10^8	13.8	293
	3.2×10^7	22.9	293
	1.4×10^7	36.7	293
	6.0×10^6	44.3	293
	5.1×10^6	54.3	293

^aZhang et al. (2015) reported 36 measurements of viscosity over the range of 0 to 60 %. For the fitting procedure, we binned their data by relative humidity and used the average viscosity and relative humidity in each bin. The width of each bin was approximately 10 % RH.

Table S6. Initial guess parameters and fitting parameters used in Eq. (1) to develop a temperature-independent parameterization for viscosity of α -pinene SOA. The fitting parameters were obtained by fitting Eq. (1) to the room-temperature viscosity data from Zhang et al. (2015) and Crittenden et al. (2012), but with the temperature (T) in Eq. (1) replaced by 293 K.

Parameter	Guess Value	Fitting Value
C_1	19	18.73
C_2	50 K	39.25
K_{GT}	2.5	0.1628
T_{gSOA}	250 K	285.9 K

Table S7. Literature viscosity data used to create a parameterization for the viscosity of sucrose particles as a function of temperature and RH.

System	Viscosity Range (Pa s)	RH (%)	Temperature (K)	Reference
Water	1.002×10^{-3} to 1.781×10^{-3}	100	275-293	Crittenden et al. (2012)

Sucrose-water	3.19×10^{-3} to 4.82×10^{-1}	96.2-80	293	Swindells et al. (1958)
	6.73×10^{-1} to 1.10×10^3	80-56.6		Quintas et al. (2006)
	1.97×10^{-3} to 5.67×10^{-2}	99.4-88		Perry and Green (2008)
	1.25×10^{-3} to 8.30×10^{-2}	99.99-87.96		Migliori et al. (2007)
	1.26×10^{-3} to 7.65×10^{-2}	99.89-87.98		Telis et al. (2007)
	1.03×10^{-3} to 5.81×10^{-2}	100-87.98		Forst et al. (2002)
	3×10^{-2} to 6.71×10^8	92-28		Power and Reid (2014)
	1×10^{12}	48.53-25.88	255-295 (5 degree increments) ^a	Zobrist et al. (2008)

^a Zobrist et al. (2008) reported glass transition temperatures as a function of water activity for the range of 160 K to 300 K. These glass transition temperatures were based on glass transition temperature measurements in the range of 180 K to 240 K, water activity measurements, and the Gordon-Taylor equation. To develop our parameterization, we used their glass transition temperatures over the range of 255 K to 295 K from their Fig. 5b, recorded in 5 K increments.

Table S8. Parameters from Zobrist et al. (2011) used in Eq. (S4) to predict the weight fractions of sucrose and water in particles as a function of relative humidity.

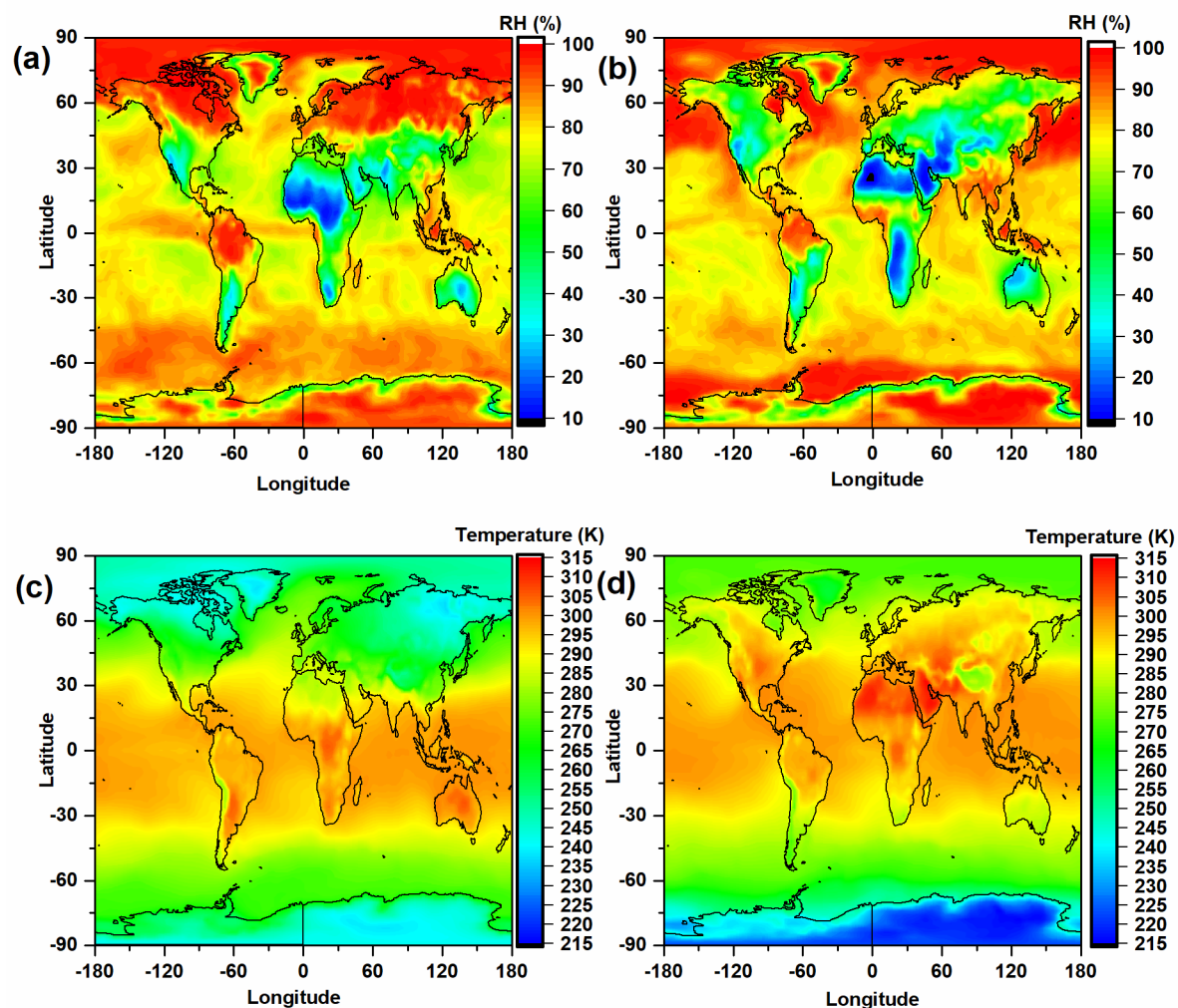
Parameter	Value	Parameter	Value
a	-1	e	-0.005151
b	-0.99721	f	0.009607
c	0.13599	g	-0.006142
d	0.001688	T ^o	298 K

Table S9. Fitting parameters used in Eq. (S3) to predict the viscosity of sucrose particles as a function of temperature and RH. These parameters were obtained by fitting Eq. (S3) to the viscosity data listed in Table S7 as well as the guess values in the table.

Parameter	Guess Value	Fitting Value
C ₁	19	20.06
C ₂	50 K	55.58 K
K _{GT}	4.74	4.531
T _{gSOA}	336 K	324.5 K

194

195 **Figures**



196

197 **Figure S1.** Monthly average relative humidity and temperature at the surface. Panels (a) and (c)
 198 correspond to January and panels (b) and (d) correspond to July.

199

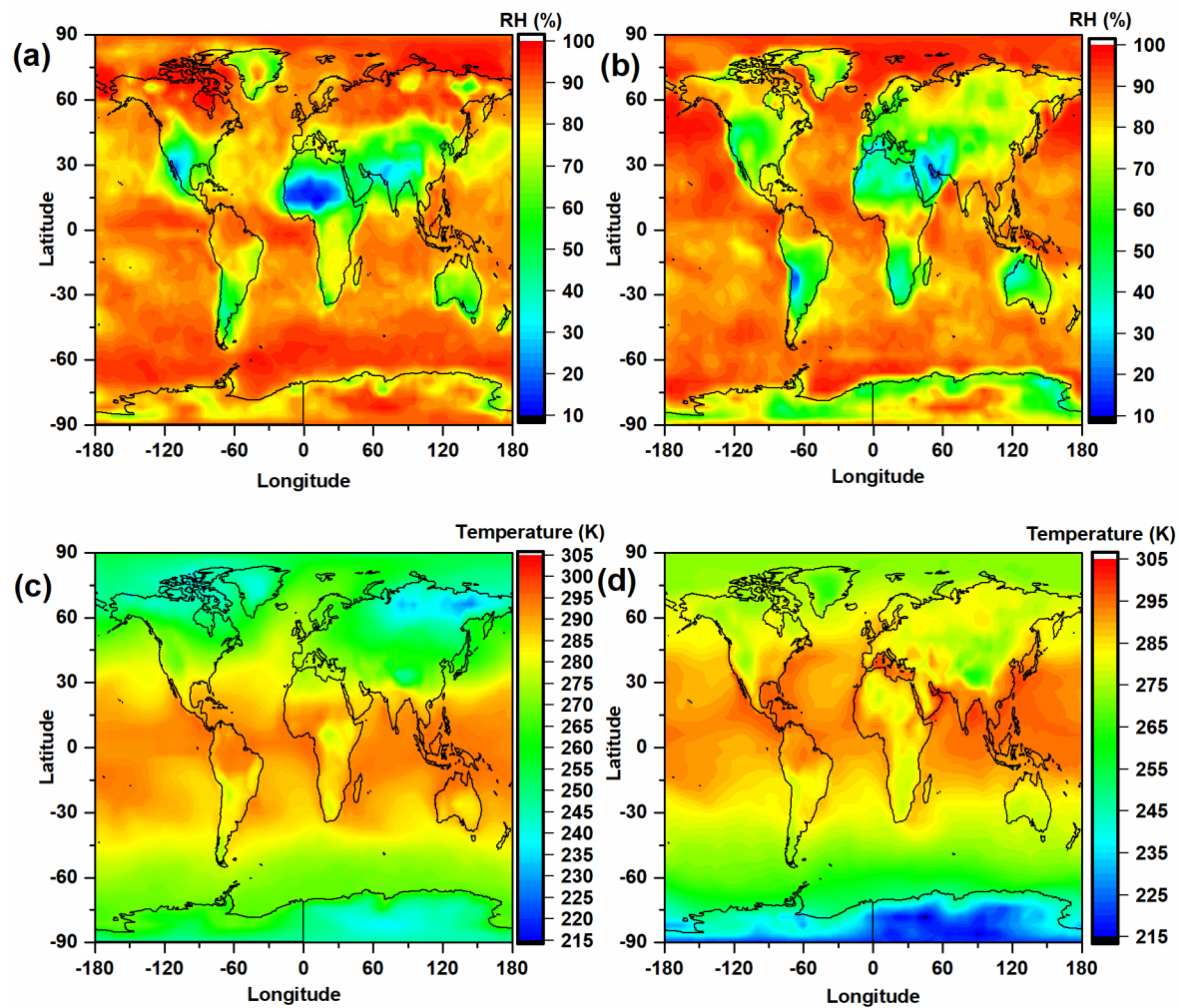


Figure S2. Monthly average relative humidity and temperature at the top of the planetary boundary layer. Panels (a) and (c) correspond to January, and panels (b) and (d) correspond to July.

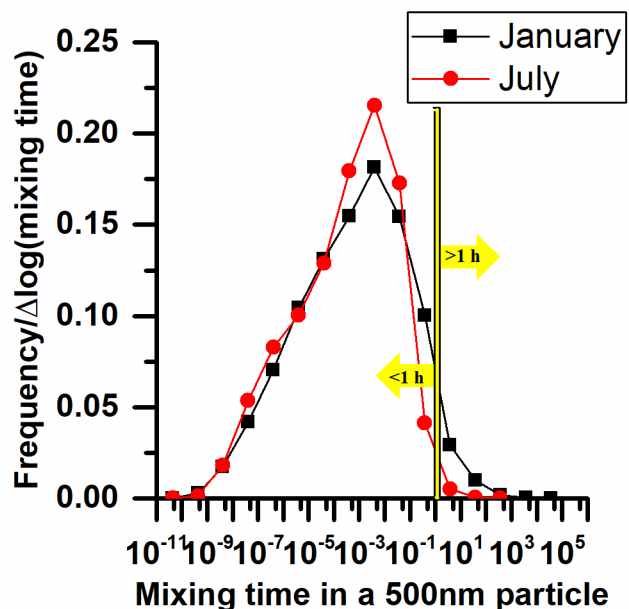


Figure S3. Normalized frequency distributions of mixing times within 500 nm α -pinene SOA in the planetary boundary layer (PBL). Black symbols correspond to January and red symbols corresponds to July. Frequency counts in the PBL were only included for the conditions where the mass concentration of total organic aerosol was $> 0.5 \mu\text{g m}^{-3}$ at the surface. The viscosity parameterization used to calculate mixing times was based on α -pinene SOA generated using mass concentrations of $\sim 1000 \mu\text{g m}^{-3}$.

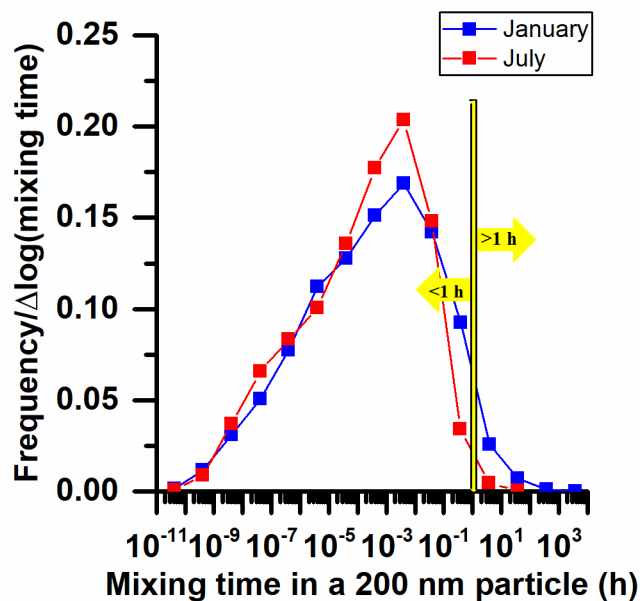
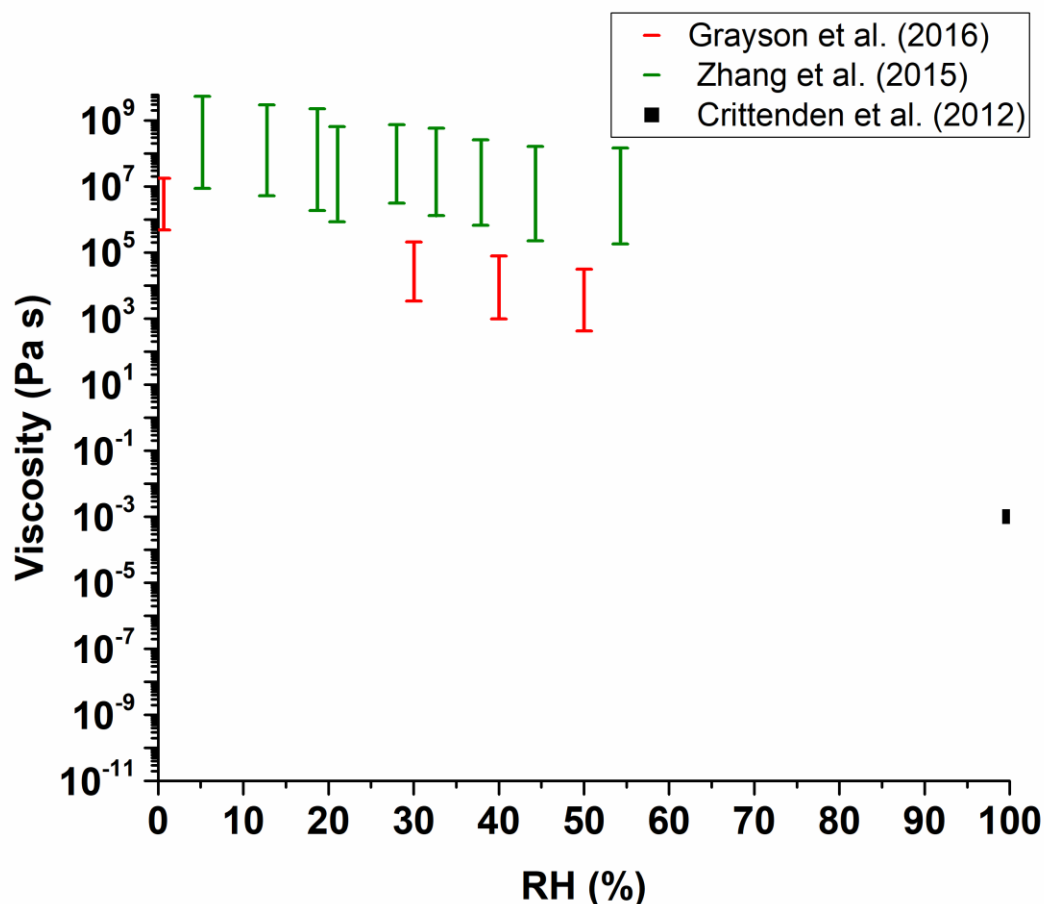


Figure S4. Normalized frequency distributions of mixing times within α -pinene SOA in the planetary boundary layer (PBL) in January for the parameterizations generated using the upper

215 limit of the viscosity data from Grayson et al. (2016) and the upper RH limit from Järvinen et al.
 216 (2016). Blue symbols correspond to January and red symbols correspond to July. Frequency
 217 counts in the PBL were only included for the conditions where the mass concentration of total
 218 organic aerosol was $> 0.5 \mu\text{g m}^{-3}$ at the surface.



219
 220 **Figure S5.** Viscosities of α -pinene particles as a function of RH from Zhang et al. (2015) and
 221 Grayson et al. (2016) as well as the viscosity of water at room temperature from Crittenden et al.
 222 (2012). The viscosity data from Grayson et al. (2016) correspond to a SOA mass concentration
 223 of $520 \mu\text{g m}^{-3}$, and the viscosity data from Zhang et al. (2015) correspond to a SOA mass
 224 concentration of $70 \mu\text{g m}^{-3}$.

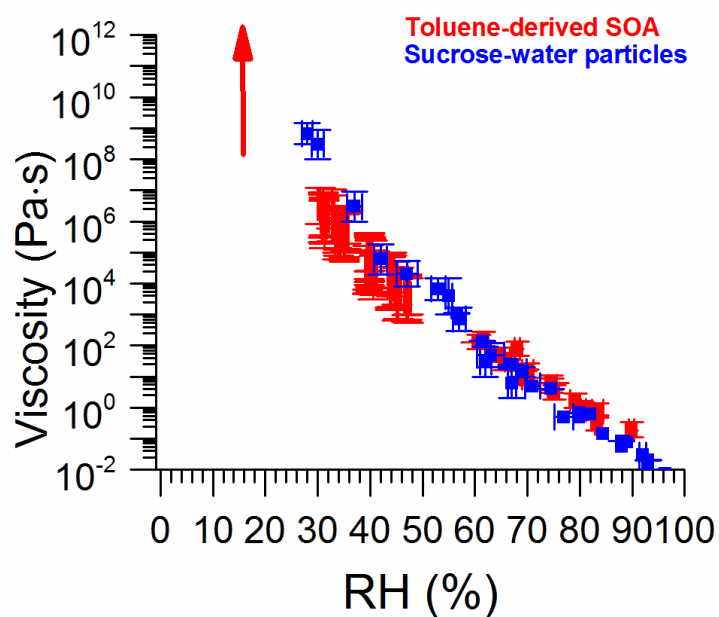


Figure S6. Viscosities of different proxies of anthropogenic SOA as a function of RH. Data for toluene SOA taken from Song et al. (2016). The data for sucrose-water mixtures was taken from Swindells (1958), Quintas et al. (2006), Telis et al. (2007), Forst et al. (2002), Migliori et al. (2007), Perry and Green (2008), and Power and Reid (2014).

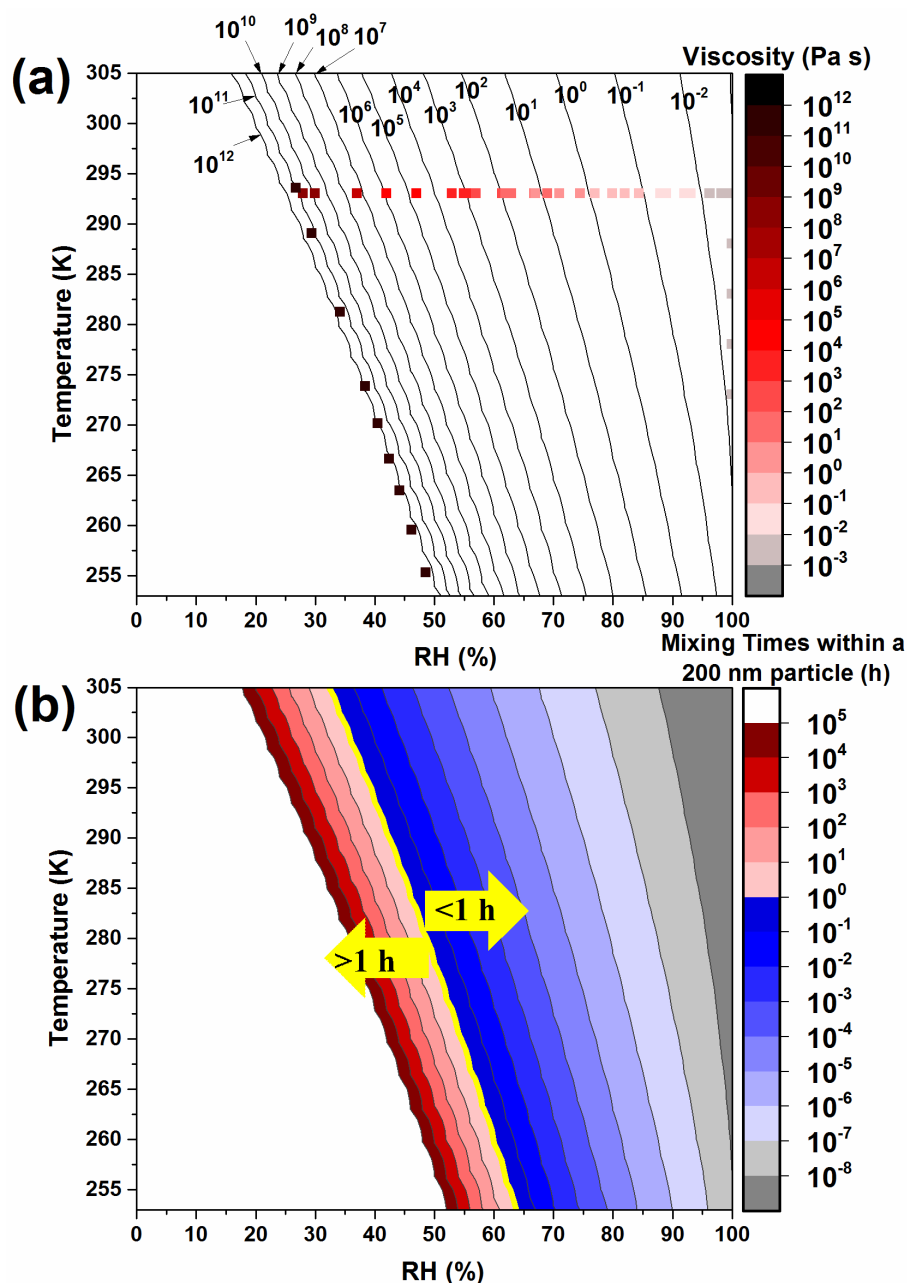
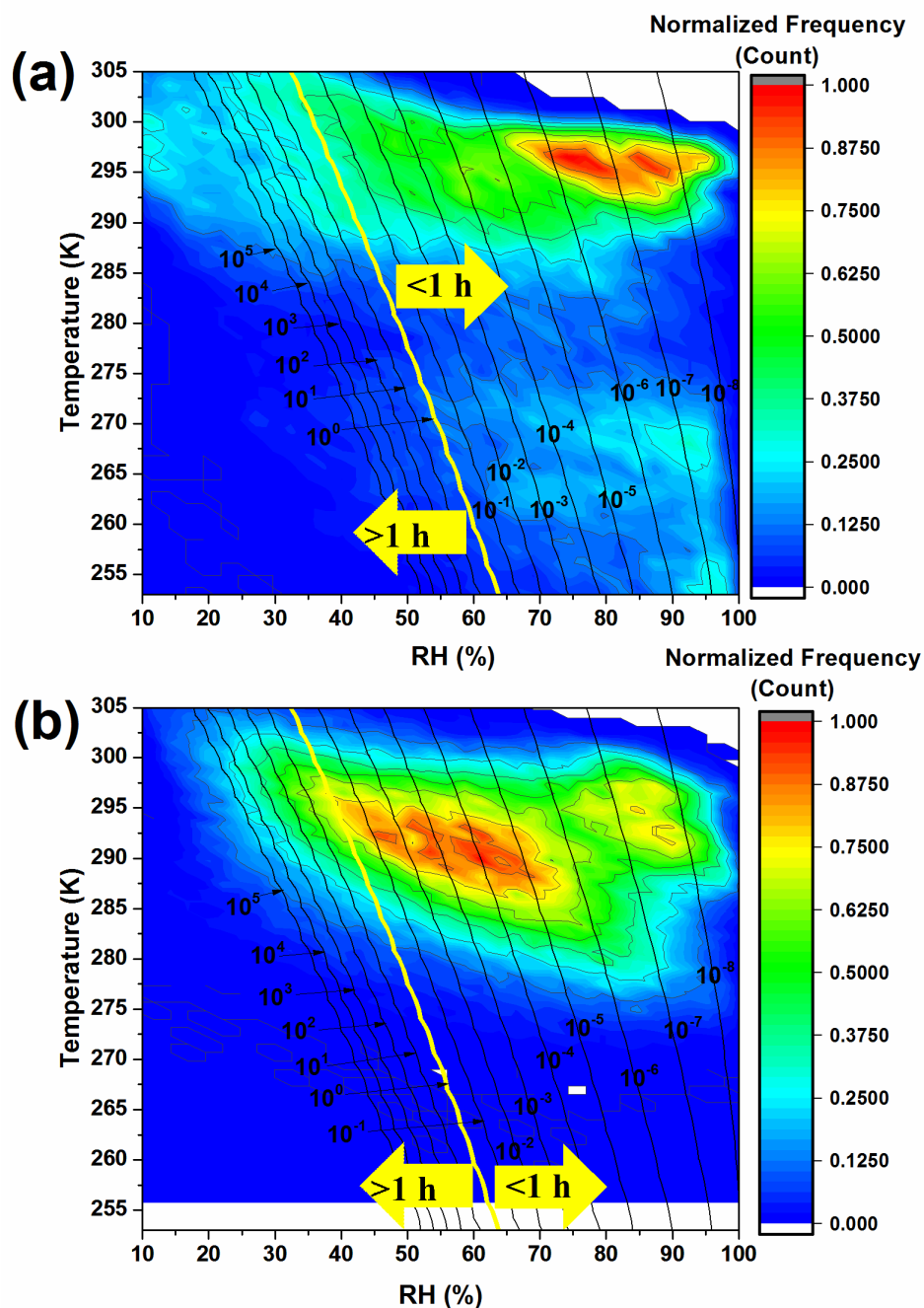
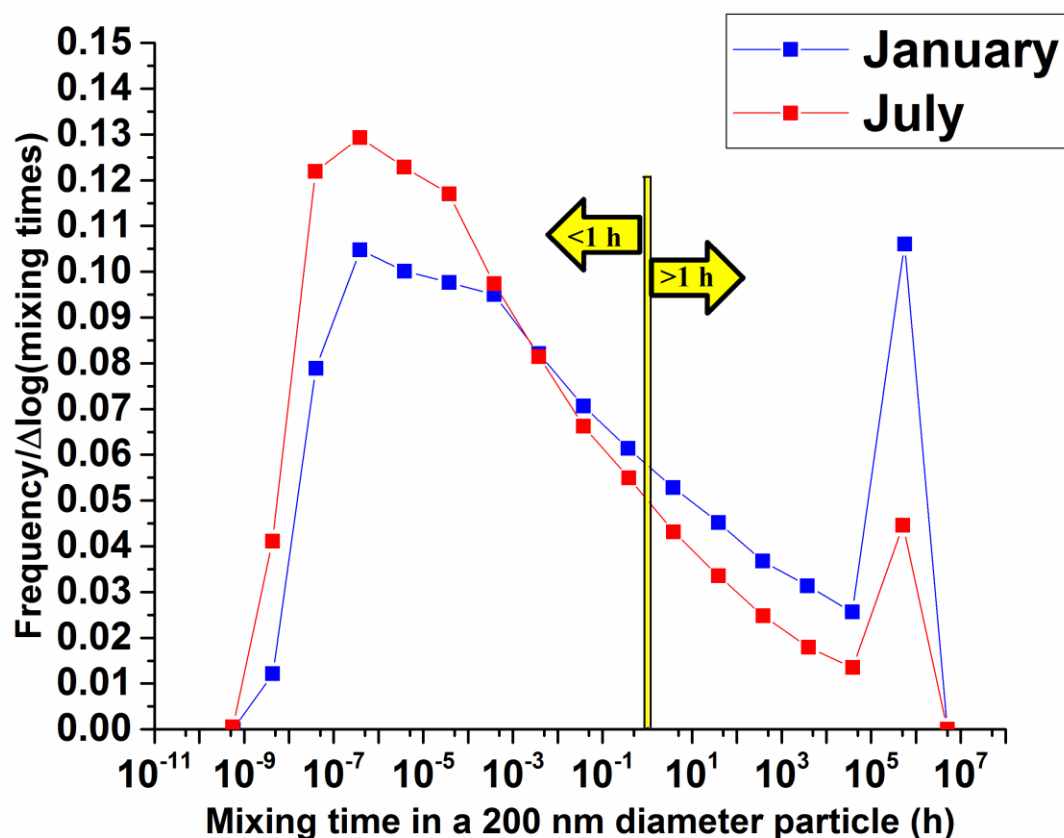


Figure S7. Panel A: Parameterization (contours) for the viscosity of sucrose particles (as surrogates of anthropogenic SOA) as a function of temperature and RH and measured viscosities used to construct the parameterization (symbols). The measured viscosities are listed in Table S7. Panel B: Mixing times (color scale) for organic molecules within 200 nm sucrose particles as a function of temperature and RH. Mixing times were calculated from the viscosity parameterization (Panel A) and Eq. (5) and (6) in the main text.



241
 242 **Figure S8.** Six-hour normalized frequency counts of temperature and RH in the planetary
 243 boundary layer (color scale) together with the mixing times for organic molecules within 200 nm
 244 sucrose particles (as surrogates of anthropogenic SOA) (contours). Panels A and B show the
 245 conditions for January and July, respectively. Mixing times (contours) are reported in hours.
 246 Frequency counts in the PBL were only included for the conditions when the mass concentration
 247 of total organic aerosol was $> 0.5 \mu\text{g}/\text{m}^3$ at the surface.



249

250 **Figure S9.** Normalized frequency distributions of mixing times within sucrose particles (as
 251 surrogates for anthropogenic SOA) in the planetary boundary layer. Red symbols correspond to
 252 January and blue symbols correspond to July. Frequency counts in the PBL were only included for
 253 the conditions where the mass concentration of total organic aerosol was $> 0.5 \mu\text{g m}^{-3}$ at the surface.
 254 The relatively large frequency count at 5×10^5 h is because all cases that had a viscosity greater
 255 than 10^{12} Pa s were assigned a value of 10^{12} Pa s. For additional details see Section S2.

256

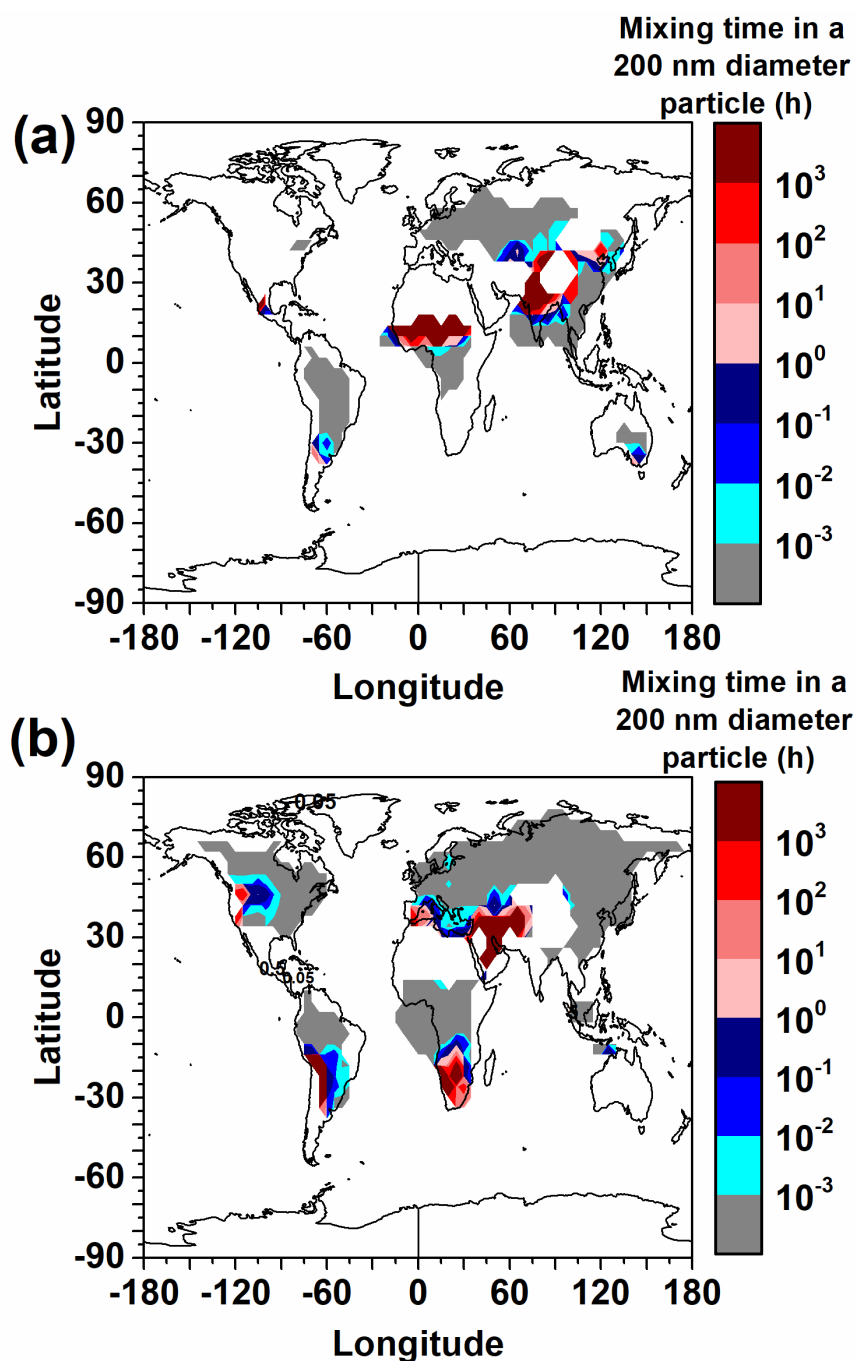


Figure S10. Mixing times of organic molecules within 200 nm sucrose particles (as surrogates of anthropogenic SOA) at the top of the planetary boundary layer as a function of latitude and longitude. The color scale represents mixing times. Mixing times are only shown for locations with total organic aerosol concentrations $> 0.5 \text{ ug m}^{-3}$ at the surface. Panels A and B correspond to January and July, respectively.